Available online at www.sciencedirect.com
SCIENCE DIRECT®
Journal of Organometallic Chemistry 666 (2003) 111–120
Journal of Organometallic Chemistry
www.elsevier.com/locate/jorganchem

# An experimental and theoretical study of the isomerization of mononuclear bis(arylselenolato)bis(triphenylphosphine)platinum complexes $[Pt(SeR)_2(PPh_3)_2]$

Milja S. Hannu-Kuure [a], Jarno Komulainen [a], Raija Oilunkaniemi [a], Risto S. Laitinen [a,*], Reijo Suontamo [b], Markku Ahlgrén [c]

[a] *Department of Chemistry, University of Oulu, P.O. Box 3000, FIN-90014 Oulu, Finland*
[b] *Department of Chemistry, University of Jyväskylä, P.O. Box 35, FIN-40350 Jyväskylä, Finland*
[c] *Department of Chemistry, University of Joensuu, P.O. Box 111, FIN-80101 Joensuu, Finland*

Received 3 September 2002; accepted 19 November 2002

## Abstract

Mononuclear bis(thienylselenolato)bis(triphenylphosphine)platinum $[Pt(SeTh)_2(PPh_3)_2]$ (Th = 2-thienyl, $C_4H_3S$) has been prepared by the treatment of *cis*-$[PtCl_2(PPh_3)_2]$ with NaSeTh. The $^{31}P$-NMR spectroscopic information indicates that *cis*-$[Pt(SeTh)_2(PPh_3)_2]$ is initially formed in the reaction. Upon prolonged standing in solution it isomerizes to *trans*-$[Pt(SeTh)_2(PPh_3)_2]$. The reaction of *cis*-$[PtCl_2(PPh_3)_2]$ with LiSeFu (Fu = 2-furyl, $C_4H_3O$) affords immediately a mixture of *cis*- and *trans*-isomers of $[Pt(SeFu)_2(PPh_3)_2]$ with the relative amount of the *trans*-isomer increasing with time. The recrystallization of the two reaction mixtures yielded *cis*,*anti*- and *trans*,*syn*-isomers of $[Pt(SeTh)_2(PPh_3)_2]$ as well as *cis,syn*- and *trans*,*anti*-isomers of $[Pt(SeFu)_2(PPh_3)_2]$. Their structures were compared with those of *cis*,*anti*- and *trans*,*anti*-isomers of $[Pt(SePh)_2(PPh_3)_2]$. The geometries and relative stabilities of all isomers of $[Pt(SeTh)_2(PH_3)_2]$, $[Pt(SeFu)_2(PH_3)_2]$ and $[Pt(SePh)_2(PH_3)_2]$ were studied by the use of ab initio molecular orbital techniques in order to model the structures and isomerization of the observed mononuclear selenolato complexes.

*Keywords:* Arylselenolato platinum complexes; X-ray crystallography; NMR spectroscopy; Ab initio MO calculations

## 1. Introduction

The transition metal complexes containing organoselenide and telluride ligands [1–5] may provide an attractive low-temperature route for binary transition metal selenides and tellurides, such as palladium and nickel selenides and tellurides [6–9] that find potential applications in materials science. It has been noted by Brennan et al. [7] that the spatial arrangement of palladium and tellurium atoms in polynuclear $[Pd_6Te_8(PEt_3)_6]$ [7] and structurally related $[Pd_6Cl_2Te_4(TeR)_2(PPh_3)_6]$ and $[Pd_6Te_4(TeR)_4(PPh_3)_6]$ (R = 2-thienyl, $C_4H_3S$ or phenyl) [10,11] resembles that in binary PdTe thus rationalizing their facile conversion. Whereas related platinum complexes do not strive for equally high nuclearity, species like $[Pt_3Te_2(Th)(PPh_3)_5]Cl$ [10] are known. It has been suggested that mononuclear chalcogenolato complexes play a significant role in the formation of such polynuclear complexes [11].

The mononuclear chalcogenolato platinum complexes can be exemplified by $[Pt(SeR)_2(PPh_3)_2]$ (R = aryl group) that can be prepared the treatment of *cis*-$[PtCl_2(PPh_3)_2]$ with NaSeR, which is obtained through reduction of $R_2Se_2$ with $NaBH_4$ [3], or by the oxidative addition of diorganodiselenides to Pt(0) centers like $[Pt(PPh_3)_4]$ [12] or $[Pt(CH_2{=}CH_2)(PPh_3)_2]$ [13]. In the solid state $[Pt(SeR)_2(PPh_3)_2]$ complexes give rise to four possible isomers.

---

* Corresponding author.

PII: S0022-328X(02)02108-3

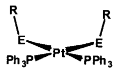

*cis, syn* (*cs*)

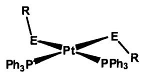

*cis, anti* (*ca*)

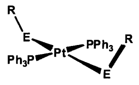

*trans, syn* (*ts*)

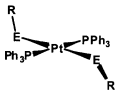

*trans, anti* (*ta*)

In solution the existence of only a *cis*- and *trans*-isomers is expected, since the organoselenolato ligands can undergo facile rotation about the Pt–Se bond. Indeed, the solution NMR spectroscopic information of different $[Pt(SeR)_2(PR_3)_2]$ complexes has been assigned in terms of the presence of *cis*- and *trans*-isomers [12–16]. It has also been suggested that the reactions starting from *cis*-$[PtCl_2(PPh_3)_2]$ initially afford the *cis*-isomer, but the product slowly isomerizes to the *trans*-isomer [12,13]. With the exception of *ca*-$[Pt(SePh)_2(PPh_3)_2]$ the X-ray structure of which has recently been reported [17], all structurally characterized $[Pt(SeR)_2(PR_3)_2]$ species with non-chelating ligands exhibit a *trans,anti* structure in the solid state [12,13,17]. The X-ray structure of a related mononuclear $[Pd(SePh)_2\{P(n\text{-}Bu)_3\}_2]$ also indicates a *ta*-isomer [18].

In the present work we report a systematic study on the structural and chemical properties of a series of $[Pt(SeR)_2(PPh_3)_2]$ (R = aryl group) complexes in light of their significance as synthons for more complicated species. While it could be expected that the structural characteristics and chemical properties of all members of the series are relatively similar regardless of the identity of the aryl group, this is not self-evident. Indeed, we have recently observed that in case of mononuclear selenoether and telluroether complexes $[MCl_2\{(C_4H_3E)E'CH_3\}_2]$ (M = Pd, Pt; E = S, O; E′ = Se, Te) the isomerism and the structures of the complexes are affected by the nature of both chalcogen atoms and aryl group both in solution and in the solid state [19]. Furthermore, whereas the crystallization of $[PdCl_2\{(C_4H_3S)SeCH_3\}_2]$ from acetone afforded the *trans*-isomer of the mononuclear complex, that of $[PdCl_2\{(C_4H_3O)SeCH_3\}_2]$ yielded a dinuclear complex $[Pd_2Cl_2(\mu\text{-}SeCH_3)_2\{CH_3Se(C_4H_2O)\}_2C(CH_3)_2]$ resulting from the condensation of the furyl groups with the solvent [20]. The reaction routes and products in the oxidative addition of diaryl dichalcogenides $R_2E_2$ (E = Se, Te) to $[M(PPh_3)_4]$ (M = Pd, Pt) are also dependent on the metal, chalcogen, aryl group, and solvent [10–12].

The different isomers of $[Pt(SeFu)_2(PPh_3)_2]$ (Fu = 2-furyl, $C_4H_3O$) (**1**) and $[Pt(SeTh)_2(PPh_3)_2]$ (Th = 2-thienyl, $C_4H_3S$) (**2**) were prepared and structurally characterized by X-ray crystallography and NMR spectroscopy. Their structures were compared with those of two $[Pt(SePh)_2(PPh_3)_2]$ (Ph = phenyl) (**3**) isomers that have been characterized previously [13,17]. We also discuss the solution equilibria of the complexes in dichloromethane and benzene. The geometries and relative stabilities of all isomers of $[Pt(SeFu)_2(PH_3)_2]$, $[Pt(SeTh)_2(PH_3)_2]$, and $[Pt(SePh)_2(PH_3)_2]$ were calculated by ab initio MO techniques in order to model the experimental data.

## 2. Experimental

### 2.1. General

All preparations were carried out under a dry argon atmosphere. As the metal complexes themselves are not sensitive to air they could be manipulated in air. *cis*-$[PtCl_2(PPh_3)_2]$ (Aldrich) and *n*-buthyl lithium (Aldrich) were used as supplied. Thiophene and furan (Aldrich) were dried on $CaCl_2$ and distilled prior to use. $Th_2Se_2$ was prepared according to the literature procedure [21,22]. Tetrahydrofuran (THF) was distilled under an argon atmosphere over Na/benzophenone. Dichloromethane, benzene, and hexane were degassed with argon.

### 2.2. X-ray crystallography

Diffraction data of *cs*-$[Pt(SeFu)_2(PPh_3)_2]$ (**1cs**), *ta*-$[Pt(SeFu)_2(PPh_3)_2]$ (**1ta**), and *ca*-$[Pt(SeTh)_2(PPh_3)_2]$ (**2ca**)[1] were collected on a Nonius Kappa CCD diffractometer using graphite monochromated Mo–$K_\alpha$ radiation ($\lambda = 0.71073$ Å) by recording 360 frames via $\varphi$-rotation ($\Delta\varphi = 1°$; twice 20–60 s per frame). Crystal data and details of structure determinations are given in Table 1.

The structures were solved by direct methods using SHELXS-97 [23] and refined using SHELXL-97 [24]. After the full-matrix least-squares refinement of non-hydrogen atoms with anisotropic thermal parameters, the hydrogen atoms were placed in calculated positions in

---

[1] A following abbreviated notation is used to describe the complexes: the bold arabic numeral refers to the molecular composition followed by two alphabets describing the isomer. In the solid state two letters are needed, i.e. **1ta** refers to *trans,anti*-$[Pt(SeFu)_2(PPh_3)_2]$. In solution only one alphabet is required, i.e. **1t** refers to *trans*-$[Pt(SeFu)_2(PPh_3)_2]$.

Table 1
Details of the structure determination of *cis,syn*-[Pt(SeFu)$_2$(PPh$_3$)$_2$] (**1cs**), *trans,anti*-[Pt(SeFu)$_2$(PPh$_3$)$_2$]·2CH$_2$Cl$_2$ (**1ta**·2CH$_2$Cl$_2$), and *cis,anti*-[Pt(SeTh)$_2$(PPh$_3$)$_2$] (**2ca**) (Fu = 2-furyl, C$_4$H$_3$O; Th = 2-thienyl, C$_4$H$_3$S)

| | **1cs** | **1ta**·2CH$_2$Cl$_2$ | **2ca** |
|---|---|---|---|
| Empirical formula | $C_{44}H_{36}O_2P_2Se_2Pt$ | $C_{23}H_{20}OPCl_2SePt_{1/2}$ | $C_{44}H_{36}P_2S_2Se_2Pt$ |
| Relative molecular mass | 1011.68 | 590.77 | 1043.80 |
| Crystal system | Monoclinic | Monoclinic | Monoclinic |
| Space group | $P2_1/n$ | $P2_1/c$ | $P2_1/n$ |
| $a$ (Å) | 11.227(2) | 11.522(2) | 11.5651(2) |
| $b$ (Å) | 15.765(3) | 12.966(3) | 15.5078(3) |
| $c$ (Å) | 21.499(4) | 15.823(3) | 21.6574(4) |
| $\beta$ (°) | 100.37(3) | 110.19(3) | 101.49(3) |
| $V$ (Å$^3$) | 3743(1) | 2218.6(8) | 3806.3(1) |
| $T$ (K) | 150(2) | 150(2) | 120(2) |
| $Z$ | 4 | 4 | 4 |
| $F(000)$ | 1968 | 1152 | 2032 |
| $D_{calc}$ (g cm$^{-3}$) | 1.795 | 1.769 | 1.821 |
| $\mu$(Mo–K$_\alpha$) (mm$^{-1}$) | 5.817 | 5.154 | 5.825 |
| Crystal size (mm) | 0.15 × 0.15 × 0.08 | 0.20 × 0.15 × 0.05 | 0.15 × 0.15 × 0.10 |
| $\theta$ Range (°) | 2.31–25.00 | 2.74–28.30 | 1.86–26.00 |
| Number of reflections collected | 48 181 | 34 655 | 31 395 |
| Number of unique reflections | 6558 | 5337 | 7477 |
| Number of observed reflections [a] | 5257 | 4665 | 5631 |
| Number of parameters | 461 | 260 | 461 |
| $R_{int}$ | 0.0737 | 0.0645 | 0.0747 |
| $R_1$ [b] | 0.0426 | 0.0375 | 0.0370 |
| $wR_2$ [b] | 0.0714 | 0.0783 | 0.0779 |
| $R_1$ (all data) | 0.0613 | 0.0479 | 0.0598 |
| $wR_2$ (all data) | 0.0763 | 0.0814 | 0.0873 |
| GOOF | 1.127 | 1.130 | 1.013 |
| Max and min heights in final difference Fourier synthesis (e Å$^{-3}$) | 0.843, −0.607 | 1.445, −1.494 | 1.347, −1.084 |

[a] $I > 2\sigma(I)$.

[b] $R_1 = \Sigma||F_o| - |F_c||/\Sigma|F_o|$, $wR_2 = [\Sigma w(F_o^2 - F_c^2)^2/\Sigma wF_o^4]^{1/2}$.

the aromatic rings (C–H = 0.95 Å). In the final refinement the hydrogen atoms were riding with the carbon atom they were bonded to. The isotropic thermal parameters of the hydrogen atoms were fixed at 1.2 times to that of the corresponding carbon atom. The scattering factors for the neutral atoms were those incorporated with the programs.

One of the thienyl groups in *ca*-[Pt(SeTh)$_2$(PPh$_3$)$_2$] (**2ca**) is disordered. The disorder was resolved by constraining the atoms C(22) and S(2) together, giving them common anisotropic temperature factors, and refining the site occupational factor. Fractional coordinates, anisotropic thermal parameters, and the full listing of bond parameters are available as Supplementary material.

### 2.3. NMR spectroscopy

The $^{31}P\{^1H\}$, $^{77}Se$ and $^{195}Pt\{^1H\}$ spectra were recorded on a Bruker DPX 400 operating at 161.98, 76.31 and 85.60 MHz, respectively. The typical respective spectral widths were 48.543, 53.333 and 51.282 kHz and the pulse widths 7.5, 6.7 and 10.0 µs. The pulse delays were 1.0, 2.0 and 0.8 s for $^{31}$P, $^{77}$Se and $^{195}$Pt, respectively. Orthophosphoric acid (85%), a saturated D$_2$O solution of selenium dioxide, and the D$_2$O solution of [PtCl$_6$]$^{2-}$ were used as external standards. The $^{31}$P and $^{195}$Pt chemical shifts are reported relative to the external standards and the $^{77}$Se chemical shifts relative to neat Me$_2$Se [$\delta(Me_2Se) = \delta(SeO_2) + 1302.6$] [25]. All spectra were measured unlocked.

### 2.4. Preparation of [Pt(SeR)$_2$(PPh$_3$)$_2$]

#### 2.4.1. [Pt(SeFu)$_2$(PPh$_3$)$_2$]

Two milliliters (5.00 mmol) of *n*-BuLi was added to a solution of 0.36 ml (5.09 mmol) of furan in 5.5 ml of THF. Selenium powder (0.395 g, 5.00 mmol) was added into the reaction solution after 30 min. After the reaction mixture was stirred at room temperature (r.t.) for further 40 min, 0.95 ml of the resulting FuSeLi solution (0.60 mmol) was added to a solution of *cis*-[PtCl$_2$(PPh$_3$)$_2$] (0.200 g, 0.25 mmol) in 20 ml of dichloromethane. After stirring of 60 min the reaction mixture was filtered and concentrated by a partial removal of the solvent. [Pt(SeFu)$_2$(PPh$_3$)$_2$] was precipitated by adding *n*-hexane to the solution. The yellow product was filtered off, washed with hexane and dried. Yield 0.198 g (78%). Anal. Calc. for C$_{44}$H$_{36}$P$_2$O$_2$Se$_2$Pt: C, 52.23; H, 3.59. Found: C, 51.54; H, 3.31%. The X-ray-quality crystals of both *cs*-[Pt(SeFu)$_2$(PPh$_3$)$_2$] (**1cs**) and *ta*-[Pt(SeFu)$_2$(PPh$_3$)$_2$] (**1ta**) were obtained by recrystallization from dichloromethane.

### 2.4.2. [Pt(SeTh)$_2$(PPh$_3$)$_2$]

NaSeTh (0.62 mmol; prepared in situ by the reduction of 0.100 g (0.31 mmol) of Th$_2$Se$_2$ in dichloromethane with a methanolic solution of NaBH$_4$) was added to a solution of 0.245 g (0.31 mmol) of *cis*-[PtCl$_2$(PPh$_3$)$_2$] in dichloromethane. The reaction mixture was stirred for 2 h at r.t., filtered, and concentrated by partial evaporation of the solvent. [Pt(SeTh)$_2$(PPh$_3$)$_2$] was precipitated by adding *n*-hexane to the solution. The orange product was filtered off, washed with hexane and dried. Yield 0.264 g (81%). Anal. Calc. for $C_{44}H_{36}P_2O_2Se_2Pt$: C, 50.63; H, 3.48; S, 6.14. Found: C, 48.97; H, 3.13; S, 5.79%. The X-ray quality crystals of *ca*-[Pt(SeTh)$_2$(PPh$_3$)$_2$] (**2ca**) were obtained by recrystallization from dichloromethane.

## 3. Computational details

Ab initio MO calculations of the twelve [Pt(SeR)$_2$-(PH$_3$)$_2$] (R = Fu, Th, Ph; see Table 2) isomers were carried out using the Stuttgart relativistic large core effective core potential approximation (RLC ECP) [26–28] by augmenting the double-zeta quality basis sets of the valence orbitals by two polarization functions for all other non-hydrogen atoms [29] except platinum for which no polarization was used (denoted below as ECP** basis). Full geometry optimizations were completed at the HF level of theory using gradient techniques. Relative energies of all isomers were explored by calculating the total energies of the molecules at the DFT level of theory involving Becke's three parameter hybrid functionals with the Perdew/Wang 91 correlation (B3PW91) [30–36] and using the HF-optimized geometries. All calculations were performed with the GAUSSIAN 98 series of programs [37].

Table 2
The abbreviated notation for [Pt(SeR)$_2$(PH$_3$)$_2$] (R = Fu, Th, Ph) isomers [a]

| | |
|---|---|
| *cs*-[Pt(SeFu)$_2$(PH$_3$)$_2$] | **4cs** |
| *cs*-[Pt(SeTh)$_2$(PH$_3$)$_2$] | **5cs** |
| *cs*-[Pt(SePh)$_2$(PH$_3$)$_2$] | **6cs** |
| *ca*-[Pt(SeFu)$_2$(PH$_3$)$_2$] | **4ca** |
| *ca*-[Pt(SeTh)$_2$(PH$_3$)$_2$] | **5ca** |
| *ca*-[Pt(SePh)$_2$(PH$_3$)$_2$] | **6ca** |
| *ts*-[Pt(SeFu)$_2$(PH$_3$)$_2$] | **4ts** |
| *ts*-[Pt(SeTh)$_2$(PH$_3$)$_2$] | **5ts** |
| *ts*-[Pt(SePh)$_2$(PH$_3$)$_2$] | **6ts** |
| *ta*-[Pt(SeFu)$_2$(PH$_3$)$_2$] | **4ta** |
| *ta*-[Pt(SeTh)$_2$(PH$_3$)$_2$] | **5ta** |
| *ta*-[Pt(SePh)$_2$(PH$_3$)$_2$] | **6ta** |

[a] *cs*, *cis,syn*; *ca*, *cis,anti*; *ts*, *trans,syn*; *ta*, *trans,anti*.

## 4. Results and discussion

### 4.1. General

The reaction of FuSeLi with *cis*-[PtCl$_2$(PPh$_3$)$_2$] in dichloromethane produces a mixture of *cis*- and *trans*-[Pt(SeFu)$_2$(PPh$_3$)$_2$] with a good combined yield. The isomers were identified by use of NMR spectroscopy. Recrystallization from dichloromethane afforded crystals of *cs*- and *ta*-[Pt(SeFu)$_2$(PPh$_3$)$_2$] that were structurally characterized by X-ray crystallography.

Mixtures of isomers of [Pt(SeR)$_2$(PPh$_3$)$_2$] (R = Th, Ph) were formed by reducing R$_2$Se$_2$ (R = Th, Ph) with NaBH$_4$ to afford RSe$^-$, which was followed by treatment with *cis*-[PtCl$_2$(PPh$_3$)$_2$] in dichloromethane or benzene. The isomers were identified by NMR spectroscopy and structurally characterized in the solid state by X-ray crystallography. The crystal structure of *ca*-[Pt(SeTh)$_2$(PPh$_3$)$_2$] has been determined in this work. Those of *ts*-[Pt(SeTh)$_2$(PPh$_3$)$_2$] [12], *ca*-[Pt(SePh)$_2$-(PPh$_3$)$_2$] [17], and *ta*-[Pt(SePh)$_2$(PPh$_3$)$_2$] [13,17] have been reported previously.

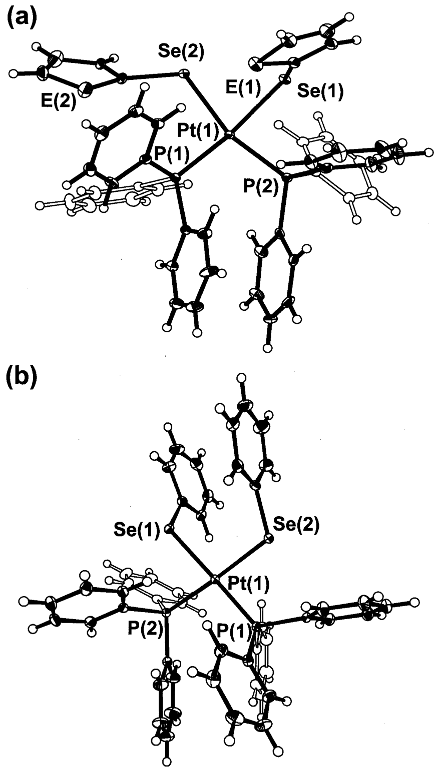

Fig. 1. The molecular structures of (a) *cs*-[Pt(SeFu)$_2$(PPh$_3$)$_2$] (**1cs**) and *ca*-[Pt(SeTh)$_2$(PPh$_3$)$_2$] (**2ca**), and (b) *ca*-[Pt(SePh)$_2$(PPh$_3$)$_2$] (**3ca**) (adapted from data in Ref. [17]) indicating the numbering of the atoms. The thermal ellipsoids have been drawn at 50% probability level.

Table 3
Selected bond lengths (Å) and angles (°) of *cs*-[Pt(SeFu)$_2$(PPh$_3$)$_2$] (**1cs**), *ta*-[Pt(SeFu)$_2$(PPh$_3$)$_2$] (**1ta**), *ca*-[Pt(SeTh)$_2$(PPh$_3$)$_2$] (**2ca**), *ts*-[Pt(SeTh)$_2$(PPh$_3$)$_2$] (**2ts**), *ca*-[Pt(SePh)$_2$(PPh$_3$)$_2$] (**3ca**), and *ta*-[Pt(SePh)$_2$(PPh$_3$)$_2$] (**3ta**)

| | **1cs** | **1ta**·2CH$_2$Cl$_2$ | **2ca** | **2ts**·1/2CH$_2$Cl$_2$ [a] | **3ca**·C$_6$H$_6$ [b] | **3ta** [b] |
|---|---|---|---|---|---|---|
| *Bond lengths* | | | | | | |
| Pt(1)−Se(1) | 2.5119(9) | 2.4535(6) | 2.5070(6) | 2.4629(1) | 2.4885(3) | 2.4525(5) |
| Pt(1)−Se(2) | 2.4675(8) | | 2.4623(6) | 2.4651(1) | 2.4506(3) | 2.4548(5) |
| Pt(1)−P(1) | 2.278(2) | 2.306(1) | 2.269(1) | 2.311(2) | 2.2900(6) | 2.325(1) |
| Pt(1)−P(2) | 2.268(2) | | 2.271(2) | 2.320(2) | 2.2937(6) | 2.314(1) |
| *Bond angles* | | | | | | |
| Se(1)−Pt(1)−Se(2) | 80.29(4) | 180.00 | 78.22(2) | 179.60(4) | 95.097(9) | 177.63(2) |
| Se(1)−Pt(1)−P(1) | 94.75(5) | 96.26(2) | 169.15(3) | 83.88(4) | 174.73(2) | 93.93(3) |
| Se(1)−Pt(1)−P(2) | 159.34(4) | 83.74(2) | 84.02(4) | 96.62(4) | 82.21(2) | 86.81(3) |
| Se(2)−Pt(1)−P(1) | 166.20(4) | 83.74(2) | 96.29(4) | 95.94(4) | 85.85(2) | 84.13(3) |
| Se(2)−Pt(2)−P(2) | 84.38(5) | 96.26(2) | 158.84(4) | 83.57(4) | 173.20(2) | 95.21(3) |
| P(1)−Pt(1)−P(2) | 103.19(6) | 180.00 | 103.03(5) | 178.20(6) | 97.40(2) | 176.41(4) |

[a] Ref. [12].
[b] Ref. [17].

## 4.2. Crystal structures

### 4.2.1. *cis*-Isomers of [Pt(SeR)$_2$(PPh$_3$)$_2$] (R = Fu, Th, Ph)

The molecular structures of *cs*-[Pt(SeFu)$_2$(PPh$_3$)$_2$] (**1cs**), *ca*-[Pt(SeTh)$_2$(PPh$_3$)$_2$] (**2ca**), and *ca*-[Pt(SePh)$_2$(PPh$_3$)$_2$] (**3ca**) [17] are shown in Fig. 1. Selected bond distances and angles are listed in Table 3.

The coordination environment around platinum in *cs*-[Pt(SeFu)$_2$(PPh$_3$)$_2$] (**1cs**) and *ca*-[Pt(SeTh)$_2$(PPh$_3$)$_2$] (**2ca**) is a slightly distorted square-plane ($\Sigma\ \alpha_{\mathrm{Pt}} = 362.1$ and 361.6° for **1cs** and **2ca**, respectively). The respective Pt−Se bond lengths for **1cs** and **2ca** [2.4675(8), 2.5119(9) and 2.4623(6), 2.5070(6) Å] are typical for single bond lengths (the sum of covalent radii of platinum and selenium is 2.46 Å [38]). They are in agreement with the Pt−Se bonds in *ca*-[Pt(SePh)$_2$(PPh$_3$)$_2$] (**3ca**) [2.4506(3), 2.4885(3) Å [17]; see Table 3] and in *cis*-[Pt(SePh)$_2$(dppm)] [2.4340(9), 2.4610(10) Å [39], and are slightly longer than those in *c*is-[Pt(Se$_2$CH$_2$)(PPh$_3$)$_2$] (2.4177(8) and 2.4352(11) Å, [40]).

Pt−P lengths also show typical single bond values in **1cs** [2.268(2), 2.278(2) Å], **2ca** [2.269(1), 2.271(1) Å], and **3ca** [2.2900(6), 2.2937(6) Å [17]]. They can be compared with the bond lengths in *cis*-[Pt(Se$_2$CH$_2$)(PPh$_3$)$_2$] and *cis*-[Pt(SePh)$_2$(dppm)] {2.274(2), 2.290(2) [40] and 2.253(2), 2.257(2) Å [22], respectively}.

Whereas **1cs** and **2ca** are nominally different isomers, they are in fact isomorphous. It can be seen in Fig. 1 that one of the selenolato groups lies approximately on the coordination plane of platinum [the torsional angle Se(1)−Pt(1)−Se(2)−C(21) shows a value of 178.2(2) and 176.1(2)° in **1cs** and **2ca**, respectively], while the other bond is almost perpendicular to the plane [the respective torsional angles Se(2)−Pt(1)−Se(1)−C(11) are −91.2(2) and +91.7(2)°]. The Se−C bond of the coplanar RSe$^-$ ligand in **1cs** and **2ca** does not lie exactly on the coordination plane of platinum but is slightly deviated. The difference in the relative signs of the torsional angles indicates that in **1cs** the two selenolato ligands lie on the same side of the coordination plane (a *cis,syn* isomer), whereas in **2ca** they are on the opposite sides (a *cis,anti* isomer).

*ca*-[Pt(SePh)$_2$(PPh$_3$)$_2$] (**3ca**) is clearly a *cis,anti*-isomer, as seen in Fig. 1(b). The torsional angles Se(1)−Pt(1)−Se(2)−C(21) and Se(2)−Pt(1)−Se(1)−C(11) show values of 61.4(8) and 65.8(2)°, respectively [17]. The same sign of the two torsional angles again imply an *anti* isomer. The molecular structure of **3ca** also differs from those of **1cs** and **2ca** by exhibiting a close contact between the phenyl rings of the *cis*-phenylselenolato ligands [C(11)···C(21) = 3.334(2) Å] [17]. In the case of **1cs** and **2ca** there are no close contacts between the two aryl groups of *cis*-selenolato ligands.

### 4.2.2. *trans*-Isomers of [Pt(SeR)$_2$(PPh$_3$)$_2$] (R = Fu, Th, Ph)

The molecular structures of *ta*-[Pt(SeFu)$_2$(PPh$_3$)$_2$] (**1ta**), *ts*-[Pt(SeTh)$_2$(PPh$_3$)$_2$] (**2ts**) [12], and *ta*-[Pt(SePh)$_2$(PPh$_3$)$_2$] (**3ta**) [17] are shown in Fig. 2. Selected bond distances and angles are listed in Table 3.

The platinum atom shows approximate square-planar coordination in each complex ($\Sigma\ \alpha_{\mathrm{Pt}} = 360.0$, 360.0 [12], and 360.6° [17] for **1ta**, **2ts**, and **3ta**, respectively). The Pt−Se bond length in **1ta** [2.4535(6) Å] is consistent with those determined previously for **2ts** and **3ta** {2.4629(1), 2.4651(1) [12] and 2.4525(5), 2.4548(5) Å [17], respectively}. These bond lengths are also consistent with other mononuclear selenolato complexes [22,40], as discussed above.

The Pt−P bond lengths in the *trans*-complexes {2.306(1) Å in **1ta**, 2.311(2), 2.320(2) Å in **2ts** [12], and 2.314(1), 2.325(1) Å in **3ta** [17]} are slightly longer than those in *cis*-complexes. This is consistent with a slightly

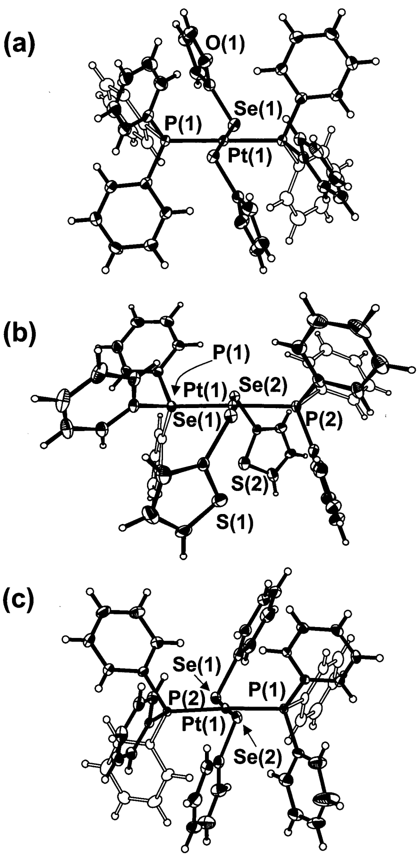

Fig. 2. The molecular structures of (a) *ta*-$[Pt(SeFu)_2(PPh_3)_2]$ (**1ta**), (b) *ts*-$[Pt(SeTh)_2(PPh_3)_2]$ [10], and (c) *ta*-$[Pt(SePh)_2(PPh_3)_2]$ [17] indicating the numbering of the atoms. The thermal ellipsoids have been drawn at 50% probability level.

stronger *trans*-influence of $PPh_3$ compared with that of the $RSe^-$ ligand.

It can be seen from Fig. 2(a) and (c) that **1ta** and **3ta** are *trans,anti*-isomers with pertinent torsional angles being 53.8(1)° {⟨P(1)–Pt(1)–Se(1)–C(1)}for **1ta**, and −24.7(5)° {⟨P(2)–Pt(1)–Se(1)–C(11)} and −151.0(5)° {⟨P(1)–Pt(1)–Se(2)–C(21)} for **3ta** [17]. By contrast **2ts** is a *trans,syn*-isomer {⟨P(1)–Pt(1)–Se(1)–C(11) = 118.94(4)–122.7(5); ⟨P(1)–Pt(1)–Se(2)–C(21) = −57.4(13)–[−60.6(3)°]} [12].

### 4.3. Optimized geometries and relative energies of the $[Pt(SeR)_2(PH_3)_2]$ ($R = Fu$, Th, Ph) isomers

The geometries and energetics of all possible isomers of $[Pt(SeR)_2(PH_3)_2]$ (see Table 2) were computed by ab initio MO techniques to explore the factors affecting the structural trends and stabilities of the observed isomers of $[Pt(SeR)_2(PPh_3)_2]$ ($R = Fu$, Th, Ph). The selected optimized bond parameters of the different isomers of $[Pt(SeR)_2(PH_3)_2]$ are shown in Table 4, and their optimized molecular geometries are shown in Fig. 3.

It is noteworthy that no local energy minimum was obtained for the *cis,syn*-isomers of $[Pt(SeFu)_2(PH_3)_2]$ (**4**) and $[Pt(SeTh)_2(PH_3)_2]$ (**5**). The optimization with different starting geometries always resulted in a *cis,anti*-isomer. In the case of $[Pt(SePh)_2(PH_3)_2]$ local minima for both **6cs** and **6ca** isomers were obtained (see Fig. 3). The existence of local minimum for the *cis,syn*-isomer can be attributed to the $\pi$-stacking of the phenyl rings of the two *cis*-phenylselenolato ligands. Such a $\pi$-stacking is missing both in the case of $[Pt(SeFu)_2(PH_3)_2]$ and $[Pt(SeTh)_2(PH_3)_2]$. The same difference has also been observed experimentally. The X-ray structure of **3ca** exhibits a close contact between the two phenyl rings of the *cis*-phenylselenolato ligands, but similar close contacts are not observed in case of **1cs** and **2ca**.

The calculated bond parameters are generally in agreement with those obtained from the crystal structure determinations (see Tables 3 and 4). The most significant deviations between the observed and calculated structures are displayed by the orientations of the selenolato ligands with respect to the plane of coordination. This can be attributed to packing effects in the

Table 4
Selected bond parameters of HF/ECP** optimized geometries of the different isomers of $[Pt(SeR)_2(PH_3)_2]$ ($R = Fu$, Th, Ph)

| | $[Pt(SeFu)_2(PH_3)_2]$ | | | $[Pt(SeTh)_2(PH_3)_2]$ | | | $[Pt(SePh)_2(PH_3)_2]$ | | | |
|---|---|---|---|---|---|---|---|---|---|---|
| | **4ca** | **4ts** | **4ta** | **5ca** | **5ts** | **5ta** | **6cs** | **6ca** | **6ts** | **6ta** |
| *Bond lengths* | | | | | | | | | | |
| Pt(1)–Se(1) | 2.51 | 2.51 | 2.53 | 2.51 | 2.51 | 2.53 | 2.53 | 2.54 | 2.52 | 2.53 |
| Pt(1)–Se(2) | 2.51 | 2.54 | 2.53 | 2.51 | 2.53 | 2.53 | 2.53 | 2.54 | 2.52 | 2.53 |
| Pt(1)–P(1) | 2.34 | 2.35 | 2.34 | 2.34 | 2.35 | 2.35 | 2.34 | 2.34 | 2.35 | 2.35 |
| Pt(1)–P(2) | 2.34 | 2.34 | 2.34 | 2.34 | 2.35 | 2.35 | 2.34 | 2.34 | 2.35 | 2.35 |
| *Bond angles* | | | | | | | | | | |
| Se(1)–Pt(1)–Se(2) | 83.2 | 177.6 | 180.0 | 82.8 | 178.7 | 180.0 | 96.0 | 95.0 | 178.8 | 180.0 |
| Se(1)–Pt(1)–P(1) | 173.6 | 87.1 | 87.7 | 173.4 | 87.4 | 87.0 | 175.7 | 177.0 | 86.7 | 87.0 |
| Se(1)–Pt(1)–P(2) | 90.0 | 95.7 | 92.3 | 90.6 | 94.5 | 93.0 | 81.9 | 82.1 | 93.3 | 93.0 |
| Se(2)–Pt(1)–P(1) | 90.5 | 91.0 | 92.3 | 90.6 | 91.5 | 93.0 | 81.9 | 82.1 | 93.3 | 93.0 |
| Se(2)–Pt(2)–P(2) | 173.2 | 86.2 | 87.7 | 173.4 | 86.7 | 87.0 | 175.7 | 177.0 | 86.7 | 87.0 |
| P(1)–Pt(1)–P(2) | 96.3 | 176.9 | 180.0 | 96.0 | 178.1 | 180.0 | 100.1 | 100.8 | 178.1 | 180.0 |

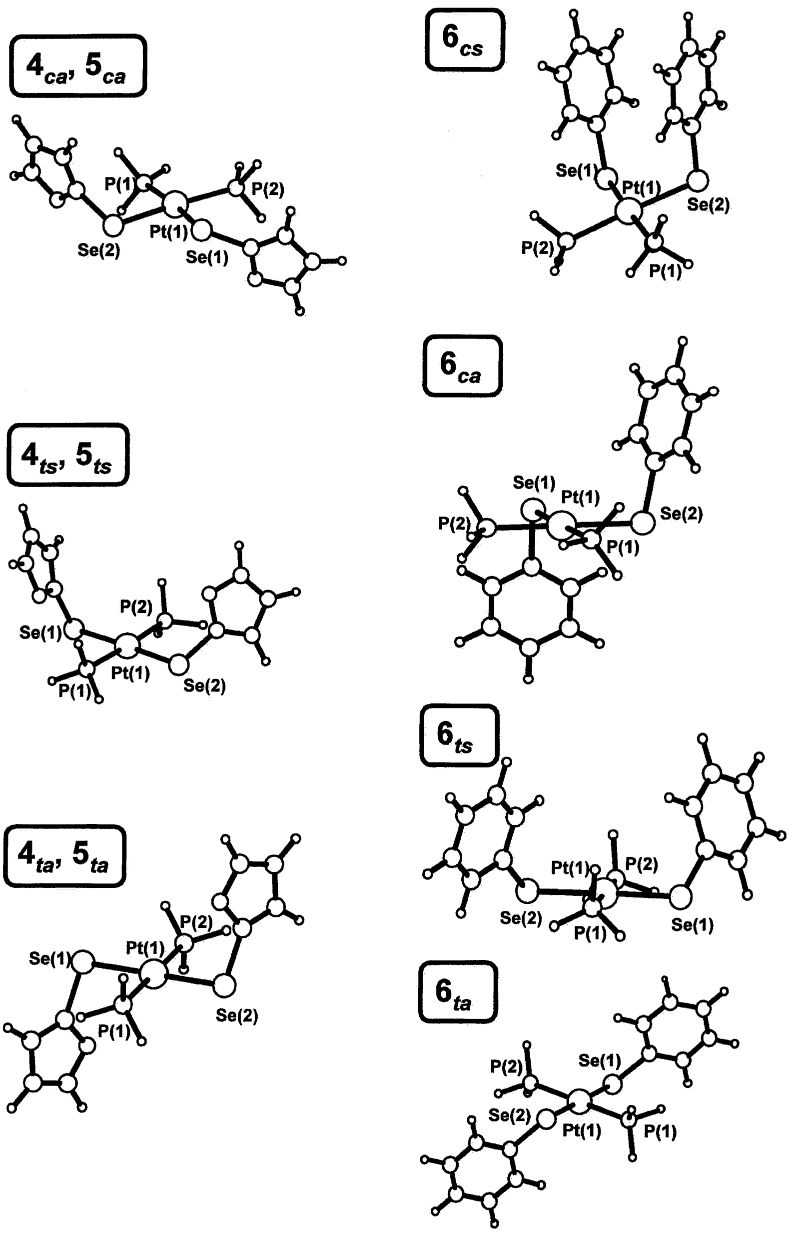

Fig. 3. The optimized HF/ECP** geometries of all isomers of $[Pt(SeR)_2(PH_3)_2]$ (R = Fu, Th, Ph).

solid state, since the NMR spectroscopic information indicates that in solution the selenolato groups can undergo virtually unhindered rotation about the Pt–Se bond [12–16].

The total HF/ECP** and B3PW91/ECP**//HF/ECP** energies of the ten isomers of $[Pt(SeR)_2(PH_3)_2]$ are listed in Table 5. They have been used to compute the relative energies of the different isomers that are shown in Fig. 4 both at HF/ECP** and B3PW91/ECP**//HF/ECP** levels of theory. It can be seen that the *cis*-isomers of all three complexes lie at a higher energy than the *trans*-isomers at both levels of theory. In every case the *cis,syn*-isomer is least stable. This is most pronounced for **4** and **5** neither of which show a local minimum for this isomer. The existence of a local minimum of *cs*-$[Pt(SePh)_2(PH_3)_2]$ (**6cs**) is probably due to the $\pi$-stacking of the selenolato phenyl rings.

We note that at B3PW91/ECP**//HF/ECP** level of theory the *cis*-isomers are predicted to be more stable relative to the *trans*-isomer than at the HF/ECP** level. The relative B3PW91/ECP**//HF/ECP** energies indicate that the *cis,anti*-isomers lie only ca. 5 kJ mol$^{-1}$ above the two *trans*-isomers in both **4** and **5**. The difference is more pronounced in the case of

Table 5
Total HF/ECP** and B3PW91/ECP**//HF/ECP** energies (in a.u.) of the $[Pt(SeR)_2(PH_3)_2]$ (R = Fu, Th, Ph) isomers

| Isomer | HF/ECP** | B3PW91/ECP** //HF/ECP** |
|---|---|---|
| *ca*-$[Pt(SeFu)_2(PH_3)_2]$ (**4ca**) | −232.06570 | −236.22137 |
| *ts*-$[Pt(SeFu)_2(PH_3)_2]$ (**4ts**) | −232.07591 | −236.22307 |
| *ta*-$[Pt(SeFu)_2(PH_3)_2]$ (**4ta**) | −232.07530 | −236.22364 |
| *ca*-$[Pt(SeTh)_2(PH_3)_2]$ (**5ca**) | −220.53630 | −224.57268 |
| *ts*-$[Pt(SeTh)_2(PH_3)_2]$ (**5ts**) | −220.54573 | −224.57472 |
| *ta*-$[Pt(SeTh)_2(PH_3)_2]$ (**5ta**) | −220.54552 | −224.57455 |
| *cs*-$[Pt(SePh)_2(PH_3)_2]$ (**6cs**) | −224.94943 | −229.30722 |
| *ca*-$[Pt(SePh)_2(PH_3)_2]$ (**6ca**) | −224.95663 | −229.31323 |
| *ts*-$[Pt(SePh)_2(PH_3)_2]$ (**6ts**) | −224.97341 | −229.32288 |
| *ta*-$[Pt(SePh)_2(PH_3)_2]$ (**6ta**) | −224.97292 | −229.32305 |

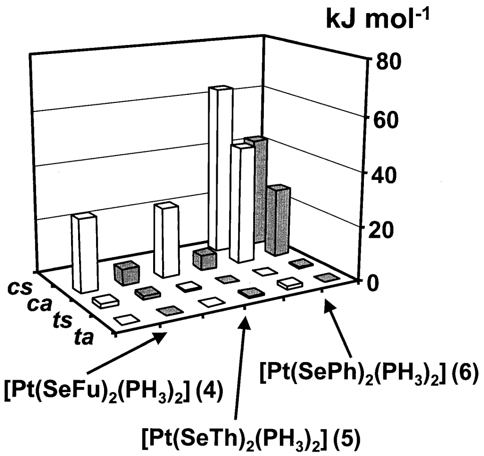

Fig. 4. Relative energies of the different isomers of $[Pt(SeR)_2(PH_3)_2]$. The white columns represent HF/ECP** energies, and the grey columns represent B3PW92/ECP**//HF/ECP** energies.

$[Pt(SePh)_2(PH_3)_2]$ (**6**) with the *cis,syn*-isomer lying at 42 kJ mol$^{-1}$ and the *cis,anti*-isomer at 26 kJ mol$^{-1}$ above the *trans,syn*- and *trans,anti*-isomers.

The *trans,syn*- and *trans,anti*-isomers show close-lying relative energies. The most stable isomers of the three complexes are *ta*-$[Pt(SeTh)_2(PH_3)_2]$, *ts*-$[Pt(SeTh)_2(PH_3)_2]$, and *ta*-$[Pt(SePh)_2(PH_3)_2]$. It is interesting to note that these computed results are in a qualitative agreement with the X-ray structures of the isolated *trans*-isomers of the three $[Pt(SeR)_2(PPh_3)_2]$ complexes: $[Pt(SeFu)_2(PPh_3)_2]$ appears as a *trans,anti*-isomer, $[Pt(SeTh)_2(PPh_3)_2]$ as a *trans,syn*-isomer, and $[Pt(SePh)_2(PPh_3)_2]$ as a *trans,anti*-isomer.

### 4.4. Isomerization of $[Pt(SeR)_2(PPh_3)_2]$

#### 4.4.1. NMR spectroscopic identification of $[Pt(SeR)_2(PPh_3)_2]$ (R = Fu, Th, Ph)

NMR spectroscopic information of the $[Pt(SeR)_2(PPh_3)_2]$ isomers is presented in Table 6. Assignment of the $^{31}P$, $^{77}Se$, and $^{195}Pt$ resonances of the isomers of $[Pt(SeTh)_2(PPh_3)_2]$ (**2**) and $[Pt(SePh)_2(PPh_3)_2]$ (**3**) was based on the trends of the chemical shifts and coupling constants, as discussed previously [12,13,17]. The resonances of $[Pt(SeFu)_2(PPh_3)_2]$ (**1**) could be assigned on the basis of the spectroscopic information from these other complexes. The assignments could be verified by redissolving the isomerically pure crystalline samples.

#### 4.4.2. Isomerization

The immediate reaction products from the reactions involving *cis*-$[PtCl_2(PPh_3)_2]$ seems to be, expectedly, *cis*-$[Pt(SeR)_2(PPh_3)_2]$. Upon prolonged standing in solution the concentration of the *cis*-isomer decreased and that of the *trans*-isomer increased. This is exemplified for $[Pt(SeTh)_2(PPh_3)_2]$ (**2**) in Fig. 5.

The calculated relative concentration of *cis*-$[Pt(SeTh)_2(PPh_3)_2]$ (**2c**) is based on the ratio of intensities of the $^{31}P$ resonances due to *cis*- and *trans*-isomers. Initially the reaction mixture shows the presence of only the *cis*-isomer, but isomerization to the *trans*-isomer proceeds quickly in the early stages of the reaction. With time the reaction becomes slower. It appears that the reaction is faster in benzene than in dichloromethane (see Fig. 5). After 500 h the $CH_2Cl_2$ and $C_6H_6$ solutions contain ca. 40 and 25 mol.% of *cis*-$[Pt(SeTh)_2(PPh_3)_2]$, respectively. The isomerization of

Table 6
NMR data for *cis*- and *trans*-isomers of $[Pt(SeR)_2(PPh_3)_2]$ (R = Fu, Th, Ph)

| | Solvent | $^{31}P\{^1H\}(\delta)$ [a] | $^{95}Pt\{^1H\}(\delta)$ [a] | $^1J(Pt–P)$ (Hz) | $^{77}Se$ $(\delta)$ [a] |
|---|---|---|---|---|---|
| *cis*-$[Pt(SeFu)_2(PPh_3)_2]$ (**1c**) | $CH_2Cl_2$ | 17.4 | −4856 | 3114 | 143 |
| *trans*-$[Pt(SeFu)_2(PPh_3)_2]$ (**1t**) | $CH_2Cl_2$ | 22.3 | −4952 | 2855 | 69 |
| *cis*-$[Pt(SeTh)_2(PPh_3)_2]$ (**2c**) [b] | $C_6H_6$ | 18.0 | −4863 | 3041 | 187 |
| *trans*-$[Pt(SeTh)_2(PPh_3)_2]$ (**2t**) [c] | $C_6H_6$ | 21.6 | −4957 | 2873 | 84 |
| *cis*-$[Pt(SePh)_2(PPh_3)_2]$ (**3c**) [d] | $C_6H_6$ | 19.1 | −4904 | 2968 | 299 |
| *trans*-$[Pt(SePh)_2(PPh_3)_2]$ (**3t**) [d] | $C_6H_6$ | 20.8 | −5040 | 2840 | 176 |

[a] In ppm.
[b] The $^{13}P$ chemical shift of **2c** in $CH_2Cl_2$ is 17.9 ppm [$^1J(Pt–P) = 3070$ Hz] [12].
[c] The $^{13}P$ chemical shift of **2t** in $CH_2Cl_2$ is 21.5 ppm [$^1J(Pt–P) = 2864$ Hz] [12].
[d] For $^{31}P$ and $^{195}Pt$-NMR spectroscopic information, see Ref. [17].

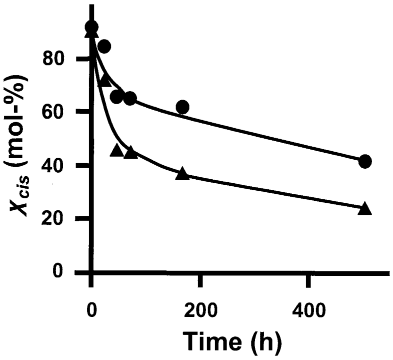

Fig. 5. Isomerization of *cis*-[Pt(SeTh)$_2$(PPh$_3$)$_2$] in $CH_2Cl_2$ (●) and $C_6H_6$ (▲). The relative content of the *cis*-isomer $\chi_{cis}$ (mol.%) has been determined from the relative intensities of the $^{31}$P resonances of *cis*- and *trans*-[Pt(SeTh)$_2$(PPh$_3$)$_2$].

*cis*-[Pt(SeFu)$_2$(PPh$_3$)$_2$] (**1c**) and *cis*-[Pt(SePh)$_2$(PPh$_3$)$_2$] (**3c**) follows qualitatively the same route as that of **2c**.

The observed isomerization from the *cis*-isomer to the *trans*-isomer is consistent with the relative energies of the different [Pt(SeR)$_2$(PH$_3$)$_2$] isomers (see Fig. 4).

## 5. Conclusions

The reaction of *cis*-[PtCl$_2$(PPh$_3$)$_2$] with RSe$^-$ in dichloromethane or benzene affords a mixture of isomers of mononuclear [Pt(SeR)$_2$(PPh$_3$)$_2$]. There are four possible isomers in the solid state for each complex. The crystal structures of *cs*-[Pt(SeFu)$_2$(PPh$_3$)$_2$], *ta*-[Pt(SeFu)$_2$(PPh$_3$)$_2$], and *ca*-[Pt(SeTh)$_2$(PPh$_3$)$_2$] were determined in this work and compared with those of *ts*-[Pt(SeTh)$_2$(PPh$_3$)$_2$], *ca*-[Pt(SePh)$_2$(PPh$_3$)$_2$], and *ta*-[Pt(SePh)$_2$(PPh$_3$)$_2$] that have been reported previously. The solution NMR spectroscopic information indicates that the selenolato ligand may undergo facile rotation about the Pt–Se bond and the actual conformation is probably determined by crystal packing. This observation is supported by ab initio MO calculations involving [Pt(SeR)$_2$(PH$_3$)$_2$] isomers as models.

The MO calculations of model [Pt(SeR)$_2$(PH$_3$)$_2$] isomers expectedly indicate that the *cis*-isomers lie at higher relative energy that the *trans*-isomers. It is consistent with the observation that upon standing in solution the *cis*-isomers of [Pt(SeR)$_2$(PPh$_3$)$_2$] isomerizes to *trans*-isomers. As shown in Fig. 5, the isomerization seems to be faster in benzene than in dichloromethane.

## 6. Supplementary material

Crystallographic information for **1cs**, **1ta**, and **2ca** (excluding tables of structure factors) have been deposited with the Cambridge Crystallographic Data Center as supplementary publication numbers CCDC 192290–192292, respectively. Copies of the data can be obtained free of charge on application to The Director, CCDC, 12 Union Road, Cambridge, CB2 1EZ, UK (Fax: +44-1223-336033; e-mail: deposit@ccdc.cam.ac.uk or www: http://www.ccdc.cam.ac.uk).

## Acknowledgements

Financial support from Academy of Finland, Finnish Cultural Foundation, Emil Aaltonen Foundation, and Tauno Tönning Foundation is gratefully acknowledged.

## References

[1] S.G. Murray, F.R. Hartley, Chem. Rev. 81 (1981) 365.
[2] H.J. Gysling, Coord. Chem. Rev. 42 (1982) 133.
[3] H. Gysling, in: S. Patai, Z. Rappoport (Eds.), The Chemistry of Organic Selenium and Tellurium Compounds, vol. I, Wiley, New York, 1986, p. 221.
[4] E.G. Hope, W. Levason, Coord. Chem. Rev. 122 (1993) 109.
[5] W. Levason, S.D. Orchard, G. Reid, Coord. Chem. Rev. 225 (2002) 159.
[6] J.G. Brennan, T. Siegrist, S.M. Stuczynski, M.L. Steigerwald, J. Am. Chem. Soc. 111 (1989) 9240.
[7] J.G. Brennan, T. Siegrist, S.M. Stuczynski, M.L. Steigerwald, J. Am. Chem. Soc. 112 (1990) 9233.
[8] M.L. Steigerwald, S.M. Stuczynski, Y.-U. Kwon, D.A. Vennos, J.G. Brennan, Inorg. Chim. Acta 312 (1993) 219.
[9] S. Dey, V.K. Jain, S. Chaudhury, A. Knoedler, F. Lissner, W. Kaim, J. Chem. Soc. Dalton Trans. (2001) 723, and references therein.
[10] R. Oilunkaniemi, R.S. Laitinen, M. Ahlgrén, J. Organomet. Chem. 595 (2000) 232.
[11] R. Oilunkaniemi, R.S. Laitinen, M. Ahlgrén, J. Organomet. Chem. 623 (2001) 168.
[12] R. Oilunkaniemi, R.S. Laitinen, M. Ahlgrén, J. Organomet. Chem. 587 (1999) 200.
[13] (a) V.K. Jain, S. Kannan, E.R.T. Tiekink, J. Chem. Res. (S) (1994) 85;
(b) V.K. Jain, S. Kannan, E.R.T. Tiekink, J. Chem. Res. (M) (1994) 0501.
[14] V. Day, D.A. Lesh, T.B. Rauchfuss, J. Am. Chem. Soc. 104 (1982) 1291.
[15] S.K. Gupta, B.L. Khandelwal, Ind. J. Chem. 29A (1990) 977.
[16] V.K. Jain, A. Singhal, S. Narayan, Phosphorus Sulphur Silicon 136–138 (1998) 483.
[17] M.S. Hannu, R. Oilunkaniemi, R.S. Laitinen, M. Ahlgrén, Inorg. Chem. Commun. 3 (2000) 397.
[18] E.C. Alyea, G. Ferguson, S. Kannan, Polyhedron 17 (1998) 2231.
[19] R. Oilunkaniemi, J. Komulainen, R.S. Laitinen, M. Ahlgrén, J. Pursiainen, J. Organomet. Chem. 571 (1998) 129.
[20] R. Oilunkaniemi, R.S. Laitinen, M. Ahlgrén, Chem. Commun. (1999) 585.
[21] L. Engman, M.P. Cava, Organometallics 1 (1982) 470.
[22] K.Y. Yen, N. Benframeno, M.P. Cava, W.S. Huang, A.G. MacDiarmid, J. Chem. Soc. Chem. Commun. (1983) 633.
[23] G.M. Sheldrick, SHELXS-97. Program for Crystal Structure Determination, University of Göttingen, Göttingen, Germany, 1997.
[24] G.M. Sheldrick, SHELXL-97. Program for Crystal Structure Refinement, University of Göttingen, Göttingen, Germany, 1997.

[25] R.C. Burns, M.J. Collins, R.J. Gillespie, G.J. Schrobilgen, Inorg. Chem. 25 (1986) 4465.
[26] W. Kuechle, M. Dolg, H. Stoll, H. Preuß, Mol. Phys. 74 (1991) 1245.
[27] A. Bergner, M. Dolg, W. Küchle, H. Stoll, H. Preuß, Mol. Phys. 80 (1993) 1431.
[28] M. Bühl, W. Thiel, U. Fleischer, W. Kutzelnigg, J. Phys. Chem. 99 (1995) 4000.
[29] S. Huzinaga (Ed.), Gaussian Basis Sets for Molecular Calculations, Physical Science Data 16, Elsevier, Amsterdam, 1984.
[30] A.D. Becke, J. Chem. Phys. 98 (1993) 5648.
[31] K. Burke, J.P. Perdew, Y. Wang, in: J.F. Dobson, G. Vignale, M.P. Das (Eds.), Electronic Density Functional Theory: Recent Progress and New Directions, Plenum, New York, 1998.
[32] J.P. Perdew, in: P. Ziesche, H. Eschrig (Eds.), Electronic Structure of Solids, Akademie Verlag, Berlin, 1991.
[33] J.P. Perdew, Y. Wang, Phys. Rev. B 45 (1992) 13244.
[34] J.P. Perdew, J.A. Chevary, S.H. Vosko, K.A. Jackson, M.R. Pederson, D.J. Singh, C. Fiolhais, Phys. Rev. B 46 (1992) 6671.
[35] J.P. Perdew, J.A. Chevary, S.H. Vosko, K.A. Jackson, M.R. Pederson, D.J. Singh, C. Fiolhais, Phys. Rev. B 48 (1993) 4978.
[36] J.P. Perdew, K. Burke, Y. Wang, Phys. Rev. B 54 (1996) 16533.
[37] M.J. Frisch, G.W. Trucks, H.B. Schlegel, G.E. Scuseria, M.A. Robb, J.R. Cheeseman, V.G. Zakrzewski, J.A. Montgomery, R.E. Stratmann, J.C. Burant, S. Dapprich, J.M. Millam, A.D. Daniels, K.N. Kudin, M.C. Strain, O. Farkas, J. Tomasi, V. Barone, M. Cossi, R. Cammi, B. Mennucci, C. Pomelli, C. Adano, S. Clifford, J. Ochterski, G.A. Petterson, P.Y. Ayala, Q. Cui, K. Morokuma, D.K. Malic, A.D. Rabuck, K. Raghavachari, J.B. Foresman, J. Ciolowski, J.V. Ortis, B.B. Stefanov, G. Liu, A. Liashenko, P. Piskorz, I. Komaromi, R. Gomperts, R.L. Martin, D.J. Fox, T. Keith, M.A. Al-Laham, C.Y. Peng, A. Nanayakkara, C. Gonzalez, M. Challacombe, P.M.W. Gill, B.G. Johnson, W. Chen, M.W. Wong, J.L. Anders, M. Head-Gordon, E.S. Replogle, J.A. Pople, GAUSSIAN 98 (Revision A.7), Gaussian Inc., Pittsburg, PA, 1998.
[38] J. Emsley, The Elements, 3rd ed, Wiley, Chichester, 1998.
[39] V.K. Jain, S. Kannan, R.J. Butcher, J.P. Jasinski, J. Chem. Soc. Dalton Trans. (1993) 1509.
[40] P.W. Khanna, C.P. Morley, M.B. Hursthouse, K.M.A. Malik, O.W. Howarth, Heteroatom Chem. 6 (1995) 519.